Study of the electrical and thermal performances of photovoltaic thermal collector-compound parabolic concentrated

Ahed Hameed Jaaz [a], Kamaruzzaman Sopian [a,*], Tayser Sumer Gaaz [b,*]

[a] Solar Energy Research Institute (SERI), Universiti Kebangsaan Malaysia, 43600 Bangi, Selangor, Malaysia
[b] Department of Machinery Equipment Engineering Techniques, Technical College Al-Musaib, Al-Furat Al Awsat Technical University, Al-Musaib, Babil 51009, Iraq

ARTICLE INFO

ABSTRACT

The importance of utilizing the solar energy as a very suitable source among multi-source approaches to replace the conventional energy is on the rise in the last four decades. The invention of the photovoltaic module (PV) could be the corner stone in this process. However, the limited amount of energy obtained from PV was and still the main challenge of full utilization of the solar energy. In this paper, the use of the compound parabolic concentrator (CPC) along with the thermal photovoltaic module (PVT) where the cooling process of the CPC is conducted using a novel technique of water jet impingement has applied experimentally and physically tested. The test includes the effect of water jet impingement on the total power, electrical efficiency, thermal efficiency, and total efficiency on CPC-PVT system. The cooling process at the maximum irradiation by water jet impingement resulted in improving the electrical efficiency by 7%, total output power by 31% and the thermal efficiency by 81%. These results outperform the recent highest results recorded by the most recent work.

Introduction

Solar energy is one of the main providers of clean and green energy throughout the continual attempts to replace the traditional energy source. There are three main research lines for developing and utilizing the solar energy: experimental, theoretical, and simulation. The experimental work focuses on developing the concentrating photovoltaic (CPC) as the main device towards establishing a larger scale of solar energy production. The work of CPC requires either collecting the highest possible solar energy to utilize it directly or converting it to electric power using photovoltaic (PV) cells. The main work on CPC includes designing new products and/or modifying the latest CPCs to optimize the solar power collection. The majority of the current installations focus on the CPC-huge size of parabolic concentrators, parabolic-trough concentrators, and Fresnel concentrators [1]. It was recorded that the use of the solar power has increased by 100 fold during the period from 2000 to 2013 to reach a capacity of 139 GW [2]. Despite this promising increase, the need for renewable technologies in general and solar PV, in particular, is a very important factor to curb the climate changes.

The promising developments of utilizing the PV solar energy are hindered by the high cost of the PV cells and low conversion efficiency (6–15%) [3]. To achieve a good solution to this dilemma, researchers are working to drop the cost of PV cells by using suitable materials and concurrently to designing new solar concentrators (CPCs) [4]. In this regard, CPCs are getting bigger in size, less in cost, and more efficient in solar energy collection [5,6]. The new designs are also fortified by using very efficient cooling techniques which are, in part, the theme of this paper.

Since the 1960s, researchers have involved in designing varieties of CPCs for building integrating systems. It was found that low concentrator PV systems are suitable due to their wide half-acceptance angle which eliminates the need for tracking of the sun [7,8] and the cooling requirements [9]. In another attempt, the maximum power output of PV module was increased by 2% by developing a flat-plate static concentrator (FPSC) [10]. It was also found that the annual power production of the non-concentrating PV was increased by 72% when CPC was involved in the design [11]. The V-trough CPC was used and the maximum power gain was up to 1.5 compared to the non-CPC system [12]. The 3-D CPC was introduced in the design and results have shown that an optical gain of 2.3-fold was achieved [13]. In another development, the dielectric material was extruded in CPC and the electrical output was doubled by 5 times [14,15]. The dielectric CPC was further improved by introducing the rotational concept and

* Corresponding authors.
  E-mail addresses: ksopian@ukm.edu.my (K. Sopian), taysersumer@gmail.com (T.S. Gaaz).

Nomenclature

A_c	frontal area solar collector (m²)	α	absorptance
b	collector width (m)	θ	collector tilt
C_P	specific heat of working fluid (J/kg °C)	ε	emittance
d	diameter of nozzle (m)	τ	transmittance
D_h	hydraulic diameter (m)	η	efficiency
F′	collector efficiency factor	σ	Stefan's Boltzmann constant (W/m² °C)
F_R	heat removal efficiency factor	a	ambient
G_r	solar radiation at NOCT (W/m²)	abs	absorber thickness
h_{fi}	heat transfer coefficient of fluid (W/m² °C)	c	cell
k	thermal conductivity (W/m °C)	f_i	inlet fluid
L	tube length (m)	g	glass
l	thickness (m)	i	inlet
·m	mass flow rate (kg/s)	j	jet
N	number of glass cover	o	outlet
p	collector perimeter (m)	p	plate
Q_u	actual useful heat gain (W)	m	mean plate
G	solar radiation (W/m²)	PV	photovoltaic
T	temperature (°C)	PVT	photovoltaic thermal
U_L	overall heat transfer coefficient (W/m² °C)	th	thermal
U_t	top loss coefficient (W/m² °C)	r	reference
v	wind velocity (m/s)	w	wind

the bare PV module has shown improvement of fold [16,17]. The asymmetric CPC was also examined and compared to normal CPC, the power concentration ratio was improved by 2.1 [18]. A new CPC construction called cross CPC was designed and found that the generated maximum power was increased by 3 times [19].

The efficiency of PV module is also influenced by the temperature. In 1978, the concept of PV-thermal (PVT) was introduced [20]. Since then, a number of experimental and simulation studies were reported [21–23]. The efficiency of the PVT with a flat collector surface was experimentally performed and verified by simulation technique [21] while the PVT with a glazed surface was tested using brine as a coolant [22]. The PVT was tested with the heat pipe and the results were very encouraging for expanding the PVT technology [23]. It was also reported that non-tracking CPC troughs are the best for normal buildings [24]. The performance of a double-pass PVT solar air CPC collector was examined with the existence of fins and the results showed that the heat dissipation from the absorber was good enough to cool down the CPC using air as coolant [25].

The debate about using a flat panel device has ended with choosing the CPC for reasons such as better efficiency, less used space, and environment. The new system was studied by several researchers aiming at evaluating the optical, thermal, and electrical efficiencies [26–28]. The results of these studies can be seen in the work of Antonini et al. [29] when PVT the maximum power attained was between 3.9 and 4.8 kW. Consequently, many systems can be designed and equipped to remove extra heat from the PV cells as a manner of cooling, which helps to enhance its efficiency due to its lowered resistance [30]. Most PVT collectors utilize water or air to cool solar cells or transfer heat to the working fluid. Huang et al. [31] proposed improvements that would result in an increased PV efficiency of 9%, thermal efficiency of 44.5%, and a total efficiency of 53.5% for the PVT collector. He et al. [32] realized a PV efficiency of 5.42%, a thermal efficiency of 51.94%, and a total efficiency of 57.38%. The experimental results show that the thermal energy for unglazed PVT system exceeds that of the glazed PVT collector. It was also seen that the efficiency of the PV cell in the case of the unglazed PVT system exceeds that of the glazed PVT collector [33]. Li et al. [34] experimentally analyzed

the performance based on the trough concentrating photovoltaic/thermal (TCPVT) system of solar cell arrays at multiple irradiance intensities. Dupeyrat et al. [35] analyzed a single glazed flat plate PVT water collector. He reported that the standard PV panel resulted in increasing thermal efficiency and decreasing electrical efficiency, which is attributed to glazing. Abu-Bakar et al. [4] analyzed the influence of asymmetrical compound parabolic concentrator on both the thermal and electrical performance, and he reported that coupling the PVT system with a concentrating PV system results in the increase of electrical output of the system. Tchinda [36] stipulated that the outlet temperature of the air is inversely related to the mass flow rate of air. It should also be pointed out that the fully covered PVT-CPC water collector system is capable of meeting the electrical and thermal demands. The electrical efficiency of partially covered PVT-CPC water collector system is inversely correlated with the solar cell temperature.

In this report, a PVT was designed as shown in Fig. 1 along with the descriptions as depicted in Table 1. The principal characters of the designed system are the use of the water jet impingent to cool down the CPC and to increase the total efficiency of the system.

Fig. 1. Photograph of PVT-CPC collector.

Table 1
Specification sheet of PV module.

Characteristic	Value
Cell type	Polycrystalline silicon
Number of cells	36 cells
Maximum power (P_{max})	135 W
Open circuit voltage (V_{oc})	21.80 V
Short circuit current (I_{sc})	7.97 A
Maximum power voltage (V_{mp})	18.12 V
Maximum power current (I_{mp})	7.45
Cell open circuit voltage	0.6 V
Module efficiency (at STC)	15%
Cell size	156×156 mm

Table 2
PVT solar collector characteristics.

Description	Symbol	Value	Unit
Ambient temperature	T_a	33	°C
Collector area	A_c	1	m^2
Number of glass cover	N	1	–
Emittance of glass	ε_g	0.88	–
Emittance of plate	ε_P	0.95	–
Collector tilt	θ	0	°
Fluid thermal conductivity	k_f	0.613	W/m °C
Specific heat of working fluid	C_P	4180	J/kg °C
Back insulation conductivity	k_b	0.045	W/m °C
Back insulation thickness	l_b	0.05	m
Insulation conductivity	k_e	0.045	W/m °C
Edge insulation thickness	l_e	0.025	m
Absorber conductivity	k_{abs}	51	W/m °C
Absorber thickness	l_{abs}	0.002	m
Transmittance	τ	0.88	–
Absorbance	α	0.95	–

Materials and methods

The water-based PVT solar collector system installed with a jet impingement and CPC. The jet impingement cooling system was made of a stainless steel tube with a diameter of 6 mm. The tubes are connected using different connectors. Fig. 2, the PVT shows the solar collector system of dimensions $1490 \times 975 \times 50$ mm. The PVT solar collector system has, at a minimum, one inlet and outlet to allow medium (water) to enter and exit from the PVT solar collector system, respectively. The jet impingement cooling system was designed and a total of 36 nozzles in order to direct jet water to the back of the PV module. The hot water is collected in a storage tank. In the current experiment, the PV module was tested. As shown in Fig. 2, the jet impingement cooling system was placed on the back of the PV module. A K-type thermocouple was used to measure the ambient and other temperatures. The thermocouple is located in multiple places and connected directly to a data logger. The mass flow rate of jet impingement can be regulated between 0.167 and 0.333 kg/s. These data will be used later to determine the performance of the system.

Experimental setup

The PVT water collector was tested at the Solar Energy Research Institute (SERI), Universiti Kebangsaan Malaysia. The control parameters (indoor test) include the PV mean, input, output and ambient temperatures, wind velocity at the collector surface, the useful current and voltage, and water jet to the PV module. The construction the PV module and CPC are displayed in Fig. 1. In this study, the PV module was constructed from 36 pieces of thin wafers of polycrystalline silicon squared array of 156 mm by 156 mm and thickness of 200 μm. Table 2 tabulates the electrical characteristic of polycrystalline silicon PV module. The jet impingement targets the back of the PV module, as shown in Fig. 2. A

total of 36 nozzles were used for jetting water to cool the back of the PV module. PVT water collectors were installed with the jet impingement system and tested in a laboratory at multiple mass flow rates of water jet impingement. The experimental setup and complete measuring system for the PVT collector are shown in Figs. 3 and 4, respectively. The experimental testing was conducted under steady-state conditions to determine the performance of the PVT system. The thermal performance of the PVT collectors can be tested by obtaining the instantaneous efficiencies of different combinations of incident solar radiation, inlet fluid temperature, outlet fluid temperature, and ambient temperature. The PVT collector with the jet impingement system was tested outdoors from 9:00 am till 4 pm. The effect of mass flow rates of 0.167, 0.25, and 0.333 kg/s were duly tested. The thermocouple was used to determine the temperatures at several points in the PVT collectors. A total of 18 thermocouples were uniformly distributed on the back of the PV module to measure the mean PV temperature. Other thermocouples were fixed on top of the PV module, water tank, inlet and outlet fluid, and at the base of the PVT collector. A data-acquisition system with 32 channels was connected to the computer system to record the data from the PVT collector, and stored every minute. The data can be used to calculate the electrical, thermal, and PVT efficiencies of the PVT collector for changing mass flow rate and solar irradiance levels. A water pump was used to activate the jet water to cool the PV module, while hot water was collected in the thermal collector and connected to the heat exchanger, and then channeled to the storage tank to form the closed-loop system.

Energy analysis

The thermal efficiency (η_{th}) and electrical efficiency (η_{ele}) for the system were duly determined, due to the fact that both are representative of the system's performance. The analytical parameters of the PVT collector are tabulated in Table 3.

The performance of the system is represented by Eq. (1) [37]:

$$\eta_{PVT} = \eta_{ele} + \eta_{th} \tag{1}$$

In the current study, the PVT system was analyzed using multiple mass flow rates. The PVT collector has assumed a flat-plate collector with a single glazing sheet. This assumption allows us to utilize the Hottel–Whillier equations to study the thermal performance of the PVT collector [37]. The thermal efficiency of a conventional flat-plate solar collector is the ratio of the useful thermal energy (Q_u) to the solar Irradiance (I), expressed by:
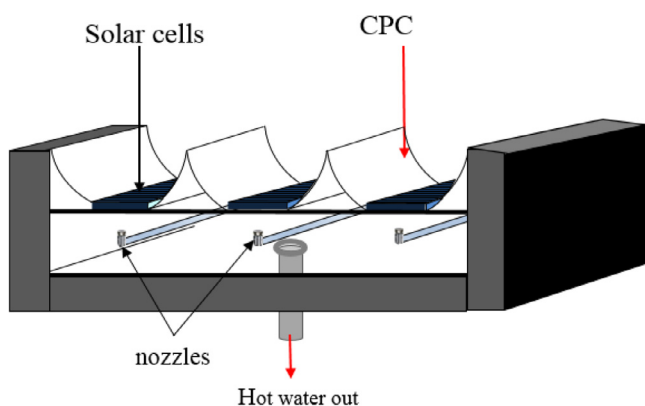
$$\eta_{th} = Q_u/I \tag{2}$$

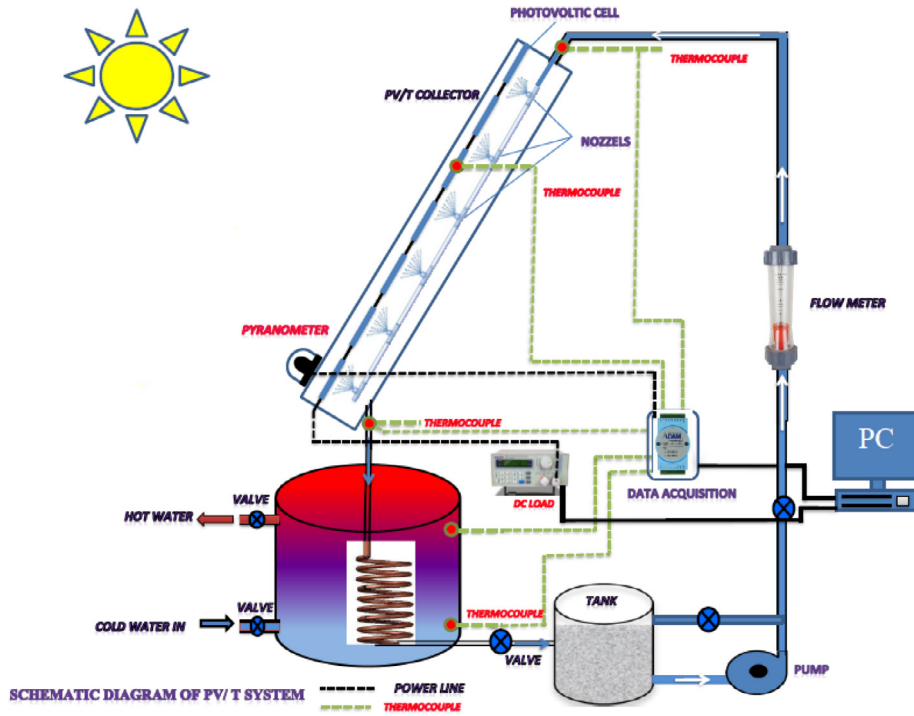**Fig. 2.** The image of the PVT-CPC collector.

Fig. 3. The schematic diagram of the PVT-CPC collector.

Fig. 4. Photograph of the experimental set-up.

Table 3
The design parameters of the PVT collector.

Parameters	Value
The length of PV module (L)	2 m
The width of PV module (W)	0.6 m
The wind velocity (v)	2 m/s
The mass flow rate of water ($\dot{m}$)	0.17 kg/s
The heat conductivity of glass cover (kg)	0.7 W/m K
The absorptivity of glass cover, ag	0.05
The number of nozzles	36 pcs
The diameter of nozzle (d)	0.001 m
The thickness of solar cell (d_c)	0.0003 m
The heat conductivity of solar cell (k_c)	148 W/m K
The spacing between nozzles to solar cell (H)	10 mm

The useful gain heat collected by the flat-plate solar collector can represent the combination of the average mass flow rate $\dot{m}$, the heat capacity of flowing medium (C_p), and temperature difference at the collector inlet (T_i), and outlet (T_o):

$$Q_u = \dot{m}C_p(T_o - T_i) \tag{3}$$

The Hottel–Whillier equation defines the difference between the absorbed solar radiation and thermal heat losses [37]:

$$Q_u = A_c F_R[G_T(\tau\alpha)_{PV} - U_L(T_i - T_a)] \tag{4}$$

where (A_c), is the collector area, (T_a), is the ambient temperature, (T_i), is the inlet temperature, (U_L), is the overall collector heat loss, (η_{PV}), is the PV thermal efficiency, (G_T), is the solar radiation at NOCT (radiation level 800 W/m^2, wind velocity 1 m/s, and ambient temperature 26 °C), and (F_R), is the heat removal efficiency factor introduced [37]. This factor is expressed as follows:

$$F_R = \frac{\dot{m}C_p}{A_c U_L}\left[1 - \exp\left(-\frac{A_C U_L F'}{\dot{m}C_p}\right)\right] \tag{5}$$

where F' is the collector efficiency factor whose values can be found in standard tables.

The overall loss coefficient (U_L), of the collector, is the sum of the edge (U_e), and top (U_t), loss coefficients, and can be expressed [37] as:

$$U_L = U_e + U_t \tag{6}$$

$$U_e = \frac{k_e pl}{L_c A_c} \tag{7}$$

$$U_t = \left[\left\{\frac{N}{\frac{C}{T_{pm}}\left[\frac{T_{pm}-T_a}{(N+f)}\right]^e} \frac{1}{h_w}\right\}^{-1} + \frac{\sigma(T_{pm}+T_a)(T_{pm}^2+T_a^2)}{(\varepsilon+0.00591Nh_w)^{-1} + \frac{2N+f-1+0.133\varepsilon_P}{\varepsilon_g} - N}\right] \tag{8}$$

where

$$C = 520(1 - 0.000051\beta^2) \tag{9}$$

$$f = (1 + 0.089h_w - 0.1166h_w\epsilon_p)(1 + 0.07866N) \qquad (10)$$

$$e = 0.43\left(1 - \frac{100}{T_{pm}}\right) \qquad (11)$$

$$T_{pm} = T_i + \frac{\frac{Q}{A_c}}{F_R U_L}(1 - F_R) \qquad (12)$$

$$T_{pm} = \frac{T_{up} + T_{bm}}{2} \qquad (13)$$

T_{pm}: Mean temperature of PV module
T_{up}: Up plate temperature

$$T_{bm} = \frac{(T_1 + T_1 + T_3 + T_4 + T_5 + T_6 + T_7 + \ldots + T_{18})}{18} \qquad (14)$$

where, T_{bm}: temperature mean back PV module where N is the number of glass covers, σ is the Stefan–Boltzmann constant, ϵ_P is the plate emittance, ϵ_g is the glass emittance, β is the collector tilt, T_{pm} is the mean plate temperature, and h_w is the wind heat-transfer coefficient. The heat transfer coefficients, such as the forced convection (h_w) can be calculated using Eq. (13), while the natural heat transfer coefficient (h_{nat}) can be calculated using Eq. (14) [37], as follows:

$$h_w = 2.8 + 3.0v \qquad (15)$$

$$h_{nat} = 1.78(T_{pm} - T_a) \qquad (16)$$

A combination of the natural and forced convection heat transfer coefficients (Eqs. (13 and 15)) determines the overall convection heat transfer (h_c) and possibly the overall top loss heat-transfer coefficient for the collector [37].

$$h_c = \sqrt{h_w^3 + h_{nat}^3} \qquad (17)$$

Eqs. (3–15) can be used to determine the useful heat gain emitted by the PVT collector. The reorientation of Eq. (3) can be used to determine the thermal efficiency of the collector [37]:

$$\eta_{th} = F_R(\tau\alpha) - F_R U_L\left(\frac{T_i - T_a}{G_T}\right) \qquad (18)$$

The electrical efficiency of the PV module (η_{PV}), which is a function of module temperature, is given by [38]:

$$\eta_{PV} = \eta_r(1 - \gamma(T_c - T_r)) \qquad (19)$$

where η_r is the reference efficiency of the PV module ($\eta_r = 0.12$), γ is a temperature coefficient ($\gamma = 0.0045$ °C), T_c is the cell temperature, and T_r is the reference temperature.

Results

Solar irradiation and ambient temperature variations

The hourly variations of the ambient temperature and solar intensity in Universiti Kebangsaan Malaysia (UKM), Bangi. The nature of this report is experimental while all relevant parameters under investigation are calculated using suitable formulas as it will be explained later. The collection of the data was carried out between 10:00 am and 4:30 pm. The solar irradiation varies with multiple parameters such as the ambient temperature, humidity, wind speed, haze, and the condition of the sky whether it is sunny or cloudy. Fig. 5(a and b) shows the solar irradiation measured in W/m² for the sunny and cloudy day where the area under the curve is reduced by 35% based on Excel calculation of the area. The measurements were restricted to the following solar irradiation: 500, 600, 700, 800, 900, and 1000 W/m² which appear

during the day in the location of this experiment. The maximum irradiation curve taken during the time of measurements is shown in Fig. 6. The solar irradiation curve is fitted using Excel-quadratic equation and the fitting curve is shown in the inset of Fig. 6. Based on the equation of fitting the distribution of the solar energy is symmetrical about the time of 1:00 pm where the azimuthal direction appears in Kuala Lumpur, Malaysia at about this time.

The other important parameter besides the variation of the solar irradiation is the variation of the ambient temperature since it influences the calculation of the efficiencies. The average temperature taken at the location of the experiment during the month of March 2016 is shown in Fig. 7. The variation of the temperature from about 29 °C in the mid-morning to about 32.5 °C around the peak. The solar irradiations and the relevant temperatures are then used precisely in the calculation using the quadratic fitting curves shown in Figs. 6 and 7 in order to have a reliable calculation. In previously reported papers where the efficiencies are calculated, there was no mentioning to consider the variation of the ambient temperature and, more likely, it was considered constant throughout the day.

The PV temperature is recorded during the time of collecting data along with the corresponding temperature due to cooling using the water impingement technique. The data show that in Fig. 8 the reduction in the temperature was 16 °C, 18 °C, and 24 °C, at 10 am, 1 pm, and 4 pm, respectively. This reduction of CPC temperatures is caused by the new cooling technique of water impingement.

Water impingement technique

The temperature of the PV-CPC system has to be reduced in order to increase the overall efficiency. To achieve this purpose, a novel approach was designed with jet impingement system. Regarding the water flow rate, the nozzle diameter was chosen at 1 mm, the flow rate was set at 0.167, 0.25 and 0.333 kg/s, and the nozzle height to the PVT-CPC module was set at 10, 20, 30 and 40 mm. The temperature was monitored by 18 thermocouples mounted at several points in the PVT collectors. Other two thermocouples were fixed at the top of PV module, water tank, and inlet and outlet fluid and at the base of PVT collector. A data-acquisition system with 32 channels was connected to the computer system to record data from PVT collector and stored every minute. This data can be used to calculate the electrical, thermal and PVT efficiencies of the PVT collector with changing mass flow rate and solar irradiance levels.

Variation of electrical, thermal, and overall efficiency of PVT

The hourly variations of electrical efficiency and cell temperature of the PVT solar collector are shown in Fig. 9. The PV cell temperature increases from 32.5 °C at 10 am, to 66.5 °C at 13:00 pm, and then decreased to 40 °C at 4:00 pm. As the temperature of the solar cell increases, the electrical efficiency decreases reaching its minimum value at the highest temperature attained of the solar cell between 12:30 and 1:30 pm. It is clearly seen that the electrical efficiency decreased from 14.5% at 10 am, to 12.25% at 1:30 pm, then increased to 14% at 4:00 pm.

Fig. 10 shows the hourly variation of electrical, thermal, and overall (PVT) efficiency for the solar collector with CPC. It can be seen that the electrical efficiency decreased from 14.5% at 10 am to 12.25% at 1:30 pm, then increased to 14% at 4:00 pm. The electrical efficiency decreases due to the PV cell temperature increase from 32.5 °C at 10 am to 66.5 °C at 13:00 pm. It can also be seen that the thermal efficiency decreases from 84% at 10 am to 81.5% at 1 pm, then to 80% at 4:00 pm. The overall efficiency is decreased
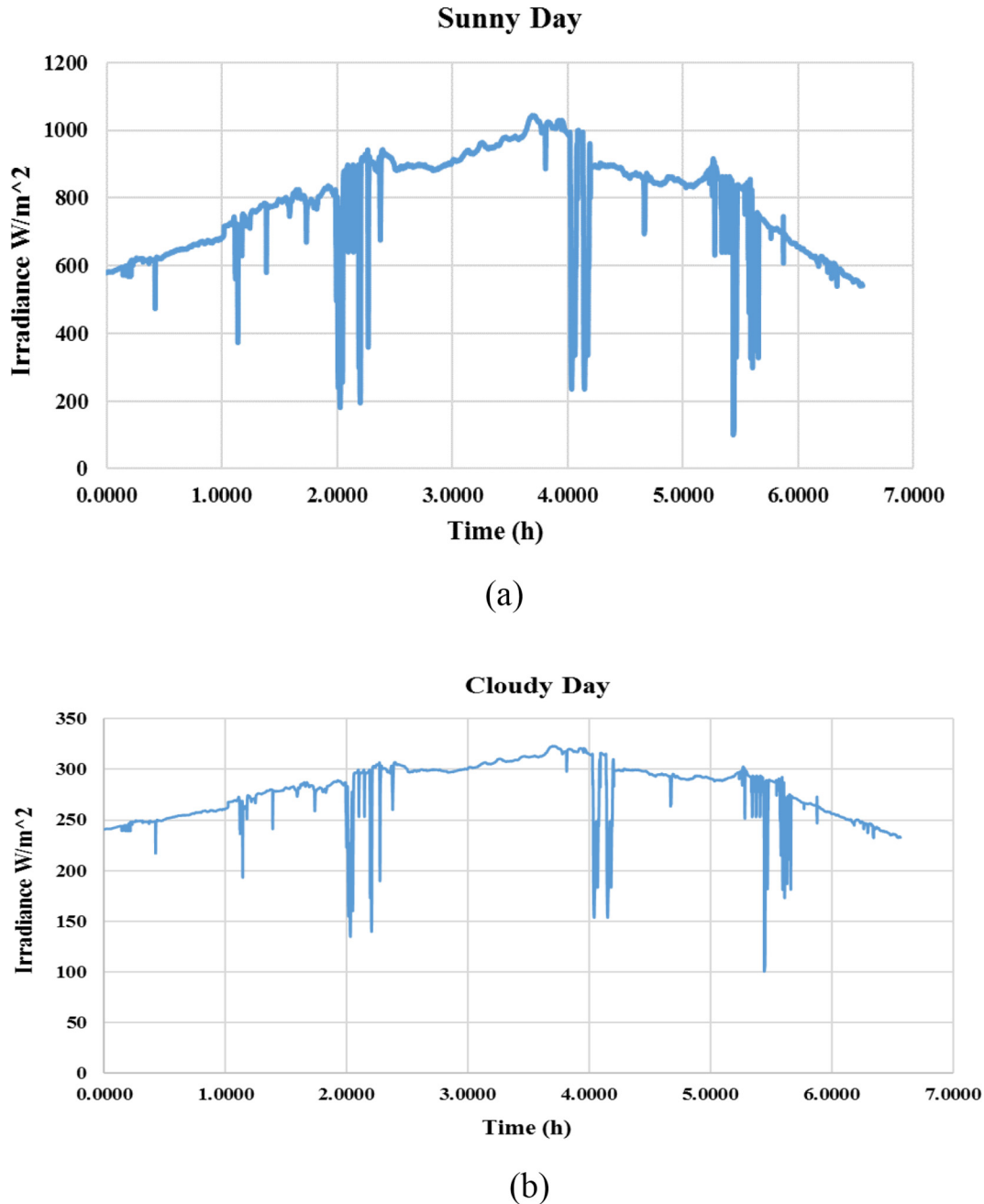
Sunny Day

(a)

Cloudy Day

(b)

Fig. 5. Irradiation during (a) sunny day and (b) cloudy day.

from 96% at 10 am, to 93% at 13:00 pm, then to 94% at 4:00 pm. The current results are in agreement with the work [32].

Effect of mass flow rate on the output power

The purpose of the water impingement is to cool down the substrate of the CPC which results in increasing the overall efficiency of the system. To achieve this purpose, the water impingement is controlled by two parameters: the mass flow rate and the height at which the nozzles are mounted beneath the CPC. Fig. 11 shows the effect of increasing the mass flow rate from 0.17 to 0.33 kg/s at a height of 10 mm. The maximum power attained at about 1 pm increased from 146 to 160 W. The increase reflects the effect of cooling the CPC. The results agree with the findings of Huang et al. [31] and Zondag et al. [39].

As a typical example, the electrical efficiency is rated at a different mass flow rate as shown in Fig. 12. The electrical efficiency of the CPC increases linearly with the increasing mass flow rate.

The performance evaluation of present PVT with jet impingement and CPC was investigated experimentally regarding the electrical and thermal efficiency of the system. Table 4 and relevant Figs. 13 and 14 show a comparative summary of PVT collector between the present study designs and other absorber collector designs. Garg and Agarwal [40] studied experimentally forced circulation flat plate solar water heater with solar cells. The experimental results of a PVT collector showed that the maximum electrical and thermal efficiencies were 8%, 49%. Huang et al. [31] suggested that further improvements achieve the electrical efficiency of 9%, a thermal efficiency of 44.5%. He et al. [32] managed to achieve the electrical efficiency of 5.42%, the thermal efficiency
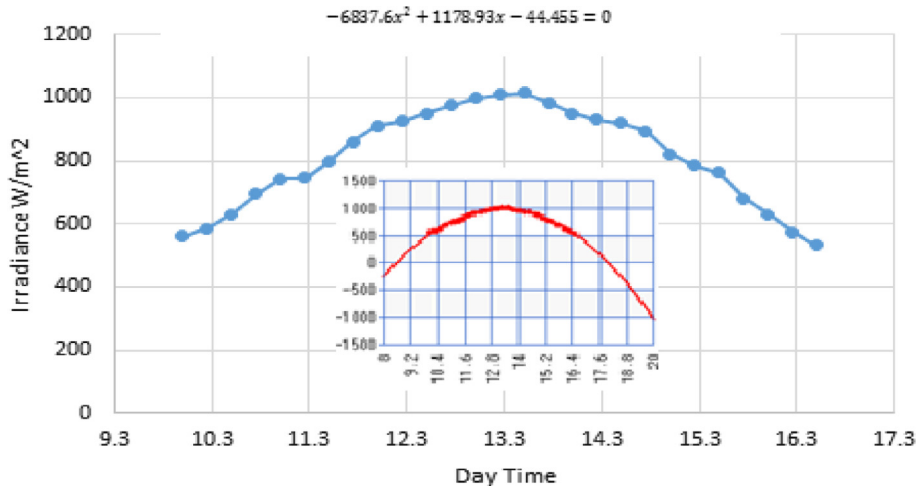
$$-6837.6x^2 + 1178.93x - 44.455 = 0$$

Fig. 6. Solar irradiation as a function of the daytime between 10:00 am and 4:00 pm.

$$y = -0.2488x^2 + 6.774x - 13.677$$
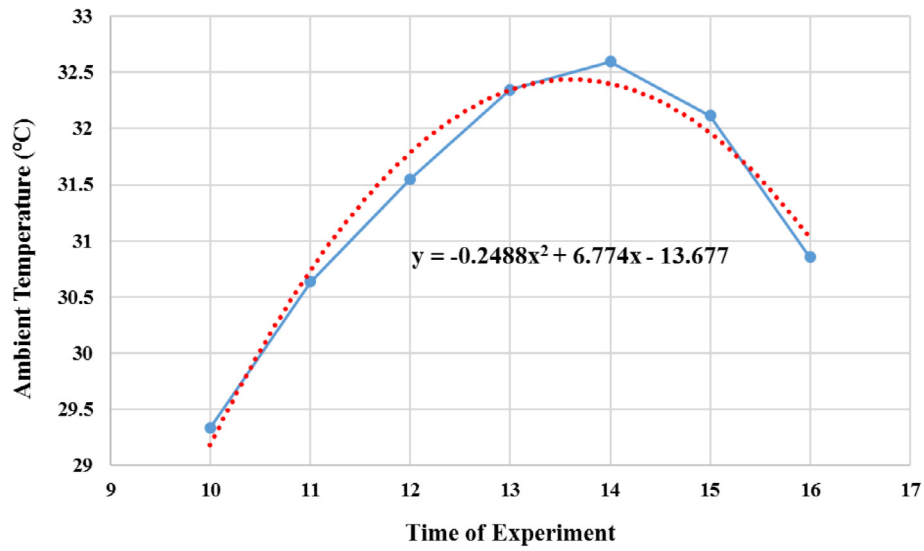
Fig. 7. The average ambient temperature at the location of the experiment during March 2016.
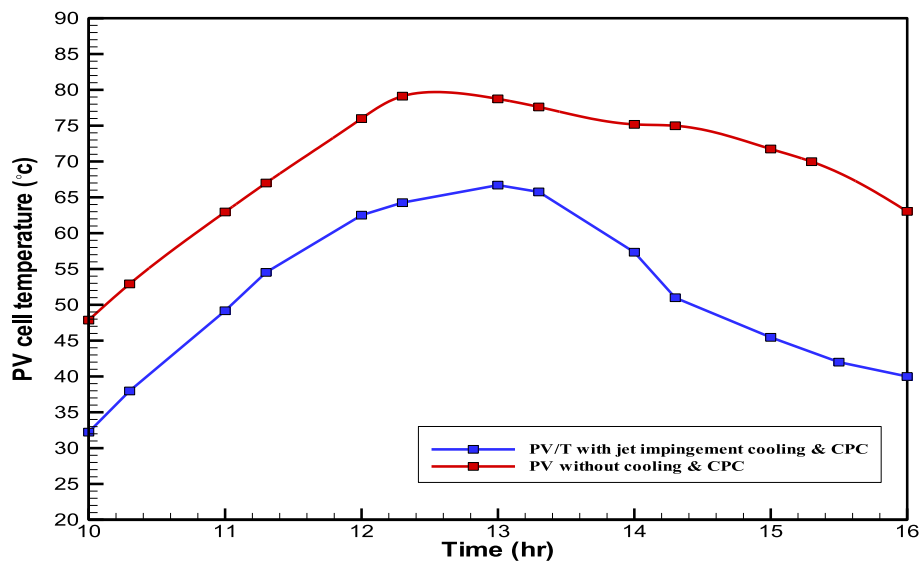

PV/T with jet impingement cooling & CPC
PV without cooling & CPC

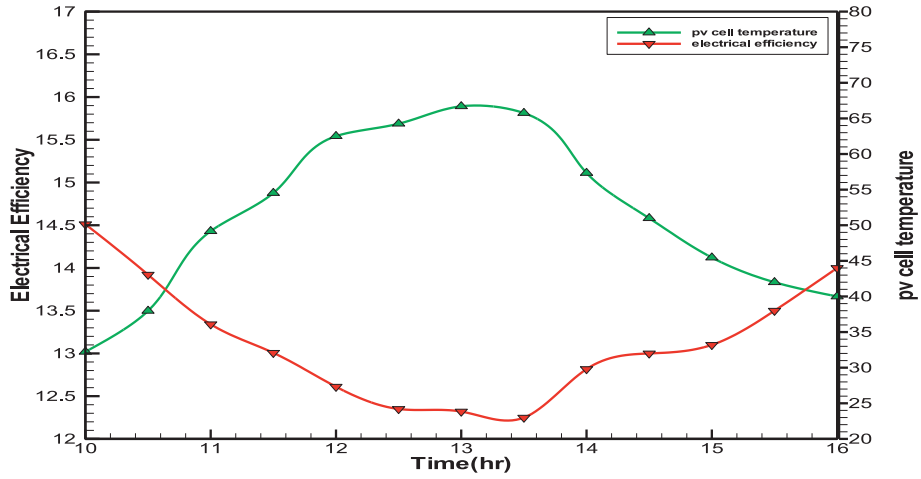**Fig. 8.** The reduction of the CPC temperature due to water impingement.

Fig. 9. The hourly variation of electrical efficiency and PV cell temperature for PVT-CPC collector.
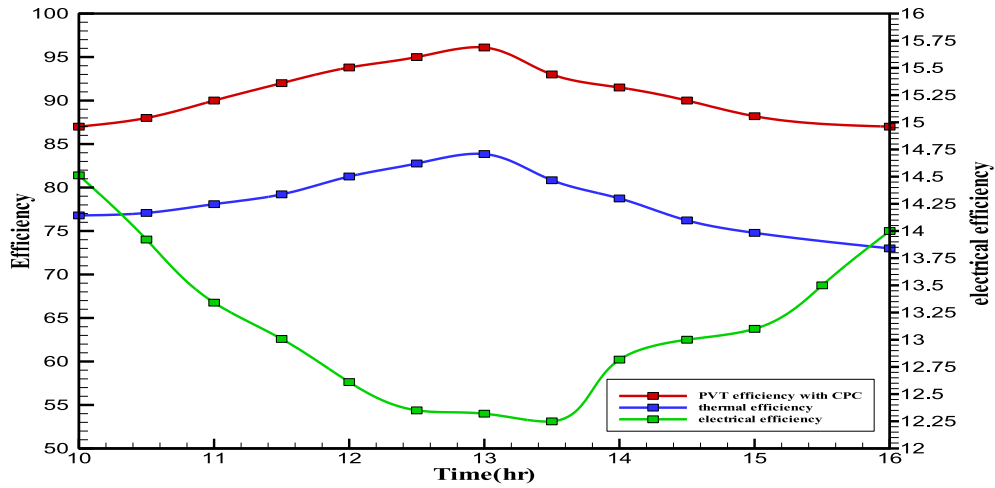

Fig. 10. The hourly variation of electrical, thermal and PVT efficiency for PVT-CPC collector.
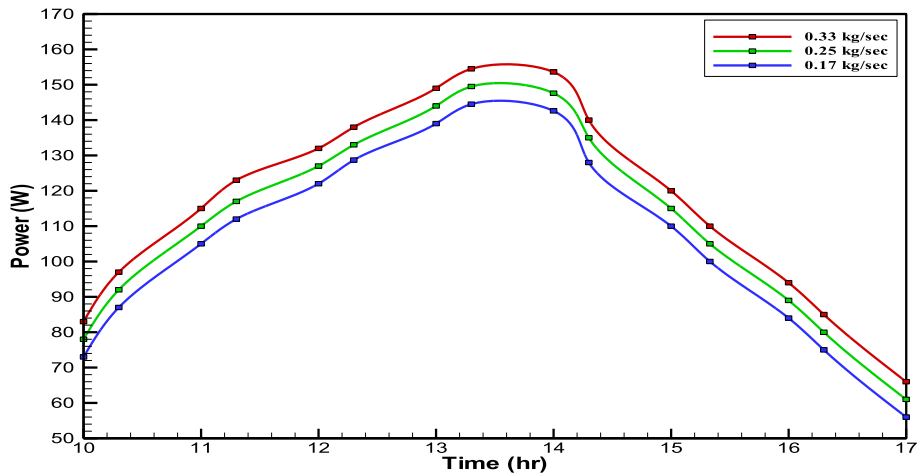

Fig. 11. The variation of the output power of PVT at three mass flow rates.
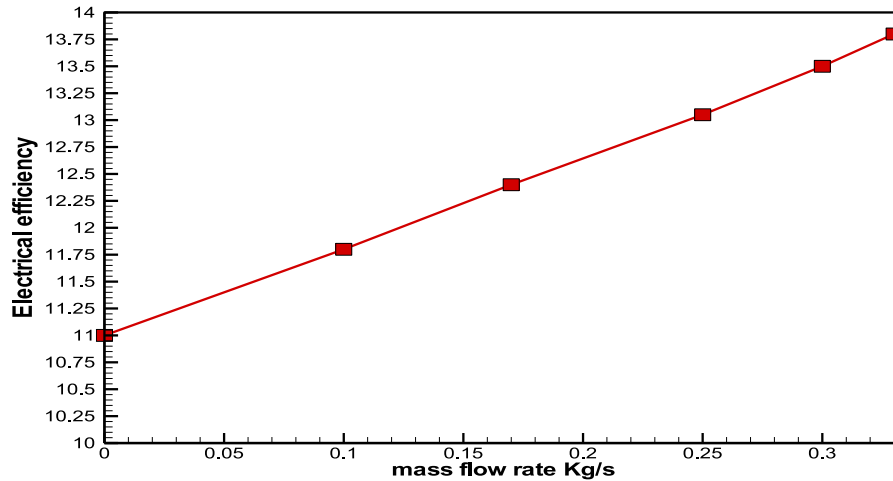
Fig. 12. The variation of electrical efficiency with mass flow rate of water for PVT-CPC collector.

Table 4
Comparison the current work with other studies in literature.

PVT collector design	η_{ele}	η_{th}	Reference
PV module with tubes, PVT	8%	49%	[40]
PV module with tubes, PVT	9%	44.5%	[31]
PV module with tubes, PVT	5.42%	51%	[32]
Sheet and tube PVT, no cover	9.7%	53%	[39]
BPVT collector	11.3%	55%	[41]
PVT collector with jet impingement and CPC	13.75%	81%	(Present Study)

of 51.94%. Zondag et al. [39] studied the electrical and thermal performance of sheet and tube for PV-thermal collectors. The electrical efficiency of 9.7%, a thermal efficiency of 63% for PVT collector with channel below transparent PV. Ibrahim et al. [41] studied experimentally the performance of BPVT. It was clearly seen that the values of the electrical efficiency and thermal efficiency are 11.3% and 51% respectively. The results of the present study of PVT collector with jet impingement with CPC shows that the maximum an electrical efficiency, thermal efficiency, and output power are 25.5%, 81%, and 9.5%, respectively.

Conclusion

In this study, an experimental investigation on PVT water collector system with jet impingement cooling and CPC was presented. The electrical performance of the PVT system with CPC was compared to a PV module. A polycrystalline silicon solar module with a jet impingent cooling system, combined with a stainless. A polycrystalline silicon solar module with the water jet impingent cooling system, combined with a stainless mirror CPC was designed, assembled, and analyzed. The experimental results showed that the integration of CPC in photovoltaic thermal collectors is superior in terms of electrical and thermal performance compared to a conventional flat plate PVT collector. Experiments were carried out to analyze the influence of jet impingement of water in PVT-CPC on both the thermal and electrical performance in addition to the output performance. The experimental results showed that the integration of CPC in PVT collectors is superior in terms of electrical and thermal performance compared to a conventional flat-PVT collector. The electrical and thermal efficiency of PVT-CPC system increased using jet impingement cooling system due to the high transfer between the back of the PV cell and cooling fluid by water jet impingement. The cooling process at the maxi-
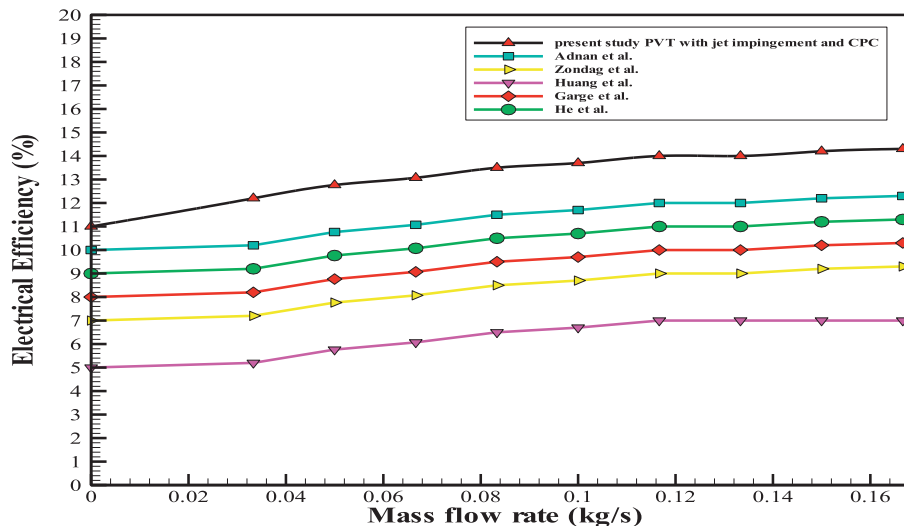

Fig. 13. Comparison electrical efficiency for PVT solar collector with jet impingement and CPC with other pervious PVT design system.
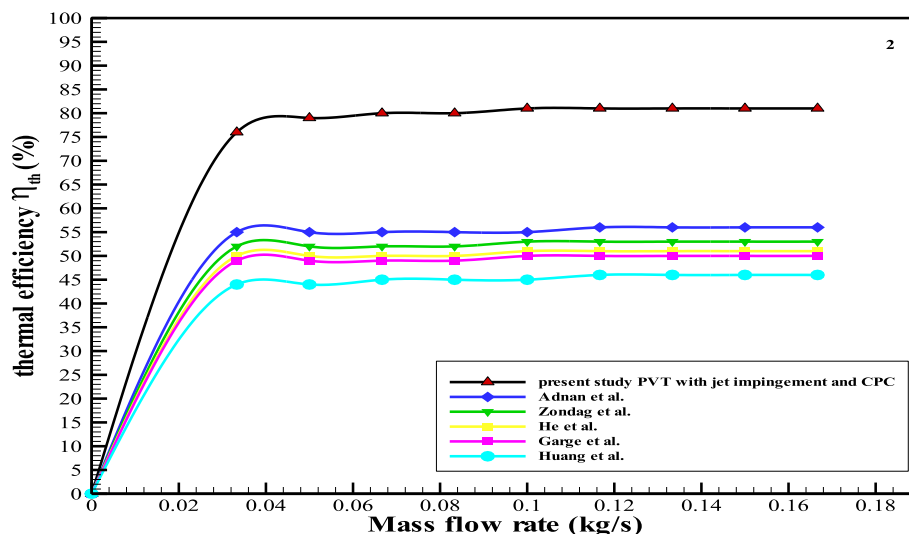
Fig. 14. Comparison thermal efficiency for PVT solar collector with jet impingement and CPC with other pervious PVT design system.

mum irradiation by water jet impingement resulted in improving the electrical efficiency by 7%, total output power by 31% and the thermal efficiency by 81%. These results outperform the recent highest results recorded by the most recent work.

Acknowledgments

Appendix A. Supplementary data

Supplementary data associated with this article can be found, in the online version, at https://doi.org/10.1016/j.rinp.2018.03.004.

References

[1] Chemisana D. Building integrated concentrating photovoltaics: a review. Renew Sustain Energy Rev 2011;15:603–11.

[2] Zheng C, Kammen DM. An innovation-focused roadmap for a sustainable global photovoltaic industry. Energy Policy 2014;67:159–69.

[3] Guiqiang L, Gang P, Su Y, Xi Z, Jie J. Preliminary study based on building-integrated compound parabolic concentrators (CPC) PV/thermal technology. Energy Proc 2012;14:343–50.

[4] Abu-Bakar SH, Muhammad-Sukki F, Freier D, Ramirez-Iniguez R, Mallick TK, Munir AB, et al. Performance analysis of a novel rotationally asymmetrical compound parabolic concentrator. Appl Energy 2015;154:221–31.

[5] Swanson RM. The promise of concentrators. Prog Photovoltaics Res Appl 2000;8:93–111.

[6] Muhammad-Sukki F, Ramirez-Iniguez R, McMeekin SG, Stewart BG, Clive B. Solar concentrators. Int J Appl Sci 2010;1:1–15.

[7] Fernández EF, Almonacid F, Sarmah N, Rodrigo P, Mallick T, Pérez-Higueras P. A model based on artificial neuronal network for the prediction of the maximum power of a low concentration photovoltaic module for building integration. Sol Energy 2014;100:148–58.

[8] Sarmah N, Richards BS, Mallick TK. Design, development and indoor performance analysis of a low concentrating dielectric photovoltaic module. Sol Energy 2014;103:390–401.

[9] Kumar NS, Matty K, Rita E, Simon W, Ortrun A, Alex C, et al. Experimental validation of a heat transfer model for concentrating photovoltaic system. Appl Therm Eng 2012;33:175–82.

[10] Uematsu T, Yazawa Y, Joge T, Kokunai S. Fabrication and characterization of a flat-plate static-concentrator photovoltaic module. Sol Energy Mater Solar Cells 2001;67:425–34.

[11] Gajbert H, Hall M, Karlsson B. Optimisation of reflector and module geometries for stationary, low-concentrating, façade-integrated photovoltaic systems. Sol Energy Mater Sol Cells 2007;91:1788–99.

[12] García M, Marroyo L, Lorenzo E, Pérez M. Experimental energy yield in 1· 5× and 2× pv concentrators with conventional modules. Prog Photovoltaics Res Appl 2008;16:261–70.

[13] Yoshioka K, Goma S, Hayakawa S, Saitoh T. Preparation and properties of an experimental static concentrator with a new three-dimensional lens. Prog Photovoltaics Res Appl 1997;5:139–45.

[14] Muhammad-Sukki F, Ramirez-Iniguez R, McMeekin S, Stewart B, Clive B. Solar concentrators in Malaysia: towards the development of low cost solar photovoltaic systems. Jurnal Teknologi 2011;55:53–65.

[15] Muhammad-Sukki F, Ramirez-Iniguez R, McMeekin S, Stewart B, Clive B. Optimised concentrator for the solar photonic optoelectronic transformer system: first optimisation stage. In: Proceedings of 2nd international conference on harnessing technology (ICHT 2011), paper. p. 1–7.

[16] Muhammad-Sukki F, Ramirez-Iniguez R, McMeekin S, Stewart B, Clive B. Optimisation of concentrator in the solar photonic optoelectronic transformer: optical gain analysis, 2011.

[17] Muhammad-Sukki F, Abu-Bakar SH, Ramirez-Iniguez R, McMeekin SG, Stewart BG, Sarmah N, et al. Mirror symmetrical dielectric totally internally reflecting concentrator for building integrated photovoltaic systems. Appl Energy 2014;113:32–40.

[18] Muhammad-Sukki F, Abu-Bakar SH, Ramirez-Iniguez R, McMeekin SG, Stewart BG, Munir AB, et al. Performance analysis of a mirror symmetrical dielectric totally internally reflecting concentrator for building integrated photovoltaic systems. Appl Energy 2013;111:288–99.

[19] Mallick TK, Eames PC. Electrical performance evaluation of low-concentrating non-imaging photovoltaic concentrator. Prog Photovoltaics Res Appl 2008;16:389–98.

[20] Kern Jr E, Russell M. Combined photovoltaic and thermal hybrid collector systems. Lexington (USA): Massachusetts Inst. of Tech., Lincoln Lab.; 1978.

[21] Raghuraman P. Analytical predictions of liquid and air photovoltaic/thermal, flat-plate collector performance. J Sol Energy Eng 1981;103:291–8.

[22] Saitoh H, Hamada Y, Kubota H, Nakamura M, Ochifuji K, Yokoyama S, et al. Field experiments and analyses on a hybrid solar collector. Appl Therm Eng 2003;23:2089–105.

[23] Pei G, Ji J, Chow TT, He H, Liu K, Yi H. Performance of the photovoltaic solar-assisted heat pump system with and without glass cover in winter: a comparative analysis. Proc Inst Mech Eng A 2008;222:179–87.

[24] Garg H, Adhikari R. Performance analysis of a hybrid photovoltaic/thermal (PV/T) collector with integrated CPC troughs. Int J Energy Res 1999;23:1295–304.

[25] Othman MYH, Yatim B, Sopian K, Bakar MNA. Performance analysis of a double-pass photovoltaic/thermal (PV/T) solar collector with CPC and fins. Renewable Energy 2005;30.

[26] Jaus J, Bett A, Reinecke H, Weber E. Reflective secondary optical elements for fresnel lens based concentrator modules. Prog Photovoltaics Res Appl 2011;19:580–90.

[27] Crisostomo F, Taylor RA, Surjadi D, Mojiri A, Rosengarten G, Hawkes ER. Spectral splitting strategy and optical model for the development of a concentrating hybrid PV/T collector. Appl Energy 2015;141:238–46.

[28] Antón I, Sala G. Losses caused by dispersion of optical parameters and misalignments in PV concentrators. Prog Photovoltaics Res Appl 2005;13:341–52.

[29] Antonini A, Butturi M, Di Benedetto P, Uderzo D, Zurru P, Milan E, et al. Rondine® PV concentrators: field results and developments. Prog Photovoltaics Res Appl 2009;17:451–9.

[30] Yao L, Damiran Z, Lim WH. Optimal charging and discharging scheduling for electric vehicles in a parking station with photovoltaic system and energy storage system. Energies 2017;10:550.

[31] Huang B, Lin T, Hung W, Sun F. Performance evaluation of solar photovoltaic/thermal systems. Solar Energy 2001;70:443–8.

[32] He W, Chow T-T, Ji J, Lu J, Pei G, Chan L-S. Hybrid photovoltaic and thermal solar-collector designed for natural circulation of water. Appl Energy 2006;83:199–210.

[33] Chow TT, Pei G, Fong K, Lin Z, Chan A, Ji J. Energy and exergy analysis of photovoltaic–thermal collector with and without glass cover. Appl Energy 2009;86:310–6.

[34] Li M, Ji X, Li G, Wei S, Li Y, Shi F. Performance study of solar cell arrays based on a trough concentrating photovoltaic/thermal system. Appl Energy 2011;88:3218–27.

[35] Dupeyrat P, Ménézo C, Rommel M, Henning H-M. Efficient single glazed flat plate photovoltaic–thermal hybrid collector for domestic hot water system. Sol Energy 2011;85:1457–68.

[36] Tchinda R. Thermal behaviour of solar air heater with compound parabolic concentrator. Energy Convers Manage 2008;49:529–40.

[37] Hottel HC, Whillier A. Evaluation of flat-plate solar-collector performance. SPIE Milestone Ser 1993;54:19–41.

[38] Al-Shamani AN, Sopian K, Mat S, Hasan HA, Abed AM, Ruslan M. Experimental studies of rectangular tube absorber photovoltaic thermal collector with various types of nanofluids under the tropical climate conditions. Energy Convers Manage 2016;124:528–42.

[39] Zondag H, De Vries D, Van Helden W, Van Zolingen R, Van Steenhoven A. The yield of different combined PV-thermal collector designs. Solar Energy 2003;74:253–69.

[40] Garg H, Agarwal R. Some aspects of a PV/T collector/forced circulation flat plate solar water heater with solar cells. Energy Convers Manage 1995;36:87–99.

[41] Ibrahim A, Othman MY, Ruslan MH, Mat S, Sopian K. Recent advances in flat plate photovoltaic/thermal (PV/T) solar collectors. Renewable Sustainable Energy Rev 2011;15:352–65.